Nuclear-Magnetic-Resonance Spin Echoes in Alloys*

H. ALLOUL AND C. FROIDEVAUX
Laboratoire de Physique des Solides,† Faculté des Sciences d'Orsay, Orsay, France
(Received 30 June 1967)

In disordered alloys, the Knight shift and the quadrupolar coupling vary from one nuclear site to the next. These variations have a strong influence on the shape of the spin-echo envelope of a given nuclear spin species. A general calculation has been developed involving 90°–180° pulse sequences. Two types of modulation of the spin-echo envelope are predicted under certain conditions. The first is related to quadrupolar effects, the second to spin-spin interactions. Experiments on Pb^{207} ($I=\frac{1}{2}$) have been performed at liquid-helium temperature in various lead solid solutions. The shape of the experimental echo envelopes agrees with the theoretical predictions. In particular, there is no dependence of the modulation period on the nature of the solute or on its concentration. The value of this period ($2\tau_M=305\pm15\ \mu$ sec) together with the exchange-narrowed linewidth in pure Pb metal is used to determine the indirect spin-spin-interaction coupling constants. The values of these coupling constants between first-nearest neighbors are, respectively, $J/2\pi=4.8$ kHz for the indirect exchange and $b/2\pi=2.2$ kHz for the pseudodipolar interaction. Similar results are analyzed for platinum. An attempt is made to interpret the results in terms of the band structure.

1. INTRODUCTION

IN nonmetallic solids, the NMR linewidth is mainly due to the dipolar interaction between nuclear spins. In metals and alloys, however, the conduction electrons induce indirect nuclear spin-spin interactions. Ruderman and Kittel[1] have shown the existence of a scalar interaction between nuclear spins, the origin of which is the contact interaction with conduction electrons. Another indirect coupling, related to the dipolar interaction between the nuclei and the electrons, was proposed by Bloembergen and Rowland.[2] Its tensorial form involves an angular dependence similar to that of pure dipolar coupling. It is therefore called the pseudodipolar coupling.

In pure metals, the NMR lineshape generally has no magnetic field dependence. The pure dipolar contribution to the linewidth is easily calculated.[3] The pseudodipolar coupling gives rise to an additional broadening. The exchange term narrows the line for like spins, but broadens it for unlike spins. Thus, various continuous-wave (cw) NMR techniques have made it possible to measure these coupling constants in some particular cases.[2,4–6] Since the spin-echo envelope is in general the Fourier transform of the absorption cw lineshape,[7] no further information is gained from spin-echo studies[8] in pure metals.

In disordered alloys, the linewidth varies strongly with the applied magnetic field. This is a consequence of the spatial variation of the electronic density[9,10] which induces a spread of the Knight shift for the different nuclei of the material as well as a distribution of quadrupolar effects. Such a microscopic distribution of the resonance frequencies changes the contribution of the spin-spin interactions to the lineshape, since the spins become "unlike". However, this cannot be observed in a cw experiment because the Knight shift and quadrupolar broadening is overwhelming. The spin-echo method partly eliminates this last broadening and thus yields results sensitive to the change of the contribution of the spin-spin couplings. This has been illustrated in Pt–Au and Pt–Ir solid solutions.[11] There the spin-echo envelopes are modulated at a frequency equal to the Ruderman-Kittel coupling constant.

Calculations of spin echoes in pure solids have been performed for the case of spin-spin interactions alone[7,12] and for the case of quadrupolar effects.[13,14] In alloys the influence of quadrupolar interactions,[15] or of the exchange coupling between nuclei of spin $\frac{1}{2}$,[11] has been studied. In the present paper, Sec. II is devoted to a more general treatment of spin-echo envelopes in alloys for 90°–180° pulse sequences. This calculation assumes that the line broadening is much larger than the contribution of the spin–spin interactions. It shows that the echo envelope can be represented by a product of two factors, one involving the quadrupolar effects and the other the spin–spin couplings. Each of these factors may have an oscillatory behavior. Experimental results obtained in some lead alloys are presented in Sec. III.

* This article covers part of the work for a "Doctorat es Sciences Physiques" thesis registered at the Centre National de la Recherche Scientifique under No. A.O. 1496, which will be submitted by H. Alloul at Orsay in 1968.

† Laboratoire associé au Centre National de la Recherche Scientifique, Paris, France.

[1] M. A. Ruderman and C. Kittel, Phys. Rev. **96**, 99 (1954).
[2] N. Bloembergen and T. J. Rowland, Phys. Rev. **97**, 1679 (1955).
[3] J. H. Van Vleck, Phys. Rev. **74**, 1168 (1948).
[4] Yu. S. Karimov and I. F. Schegolev, Zh. Eksperim. i Teor. Fiz. **41**, 1082 (1961) [English transl.: Soviet Phys.—JETP **14**, 772 (1962).
[5] J. Poitrenaud and J. M. Winter, J. Phys. Chem. Solids **25**, 123 (1964).
[6] J. Poitrenaud, J. Phys. Chem. Solids **28**, 161 (1967).
[7] I. J. Lowe and R. E. Norberg, Phys. Rev. **107**, 46 (1957).
[8] E. L. Hahn, Phys. Rev. **80**, 580 (1950).
[9] A. Blandin, E. Daniel, and J. Friedel, Phil. Mag. **4**, 180 (1959).
[10] A. Blandin and E. Daniel, J. Phys. Chem. Solids **10**, 126 (1959).
[11] C. Froidevaux and M. Weger, Phys. Rev. Letters **12**, 123 (1964).
[12] B. Herzog and E. L. Hahn, Phys. Rev. **103**, 148 (1956).
[13] I. Solomon, Phys. Rev. **110**, 61 (1958).
[14] H. Abe, H. Yasuoka, and A. Hirai, J. Phys. Soc. Japan **21**, 77 (1966).
[15] J. Butterworth, Proc. Phys. Soc. (London) **86**, 297 (1965).

In these systems, both indirect couplings were thought to be of the same order of magnitude.[16] The spin-echo envelopes are found to be modulated. Several features of the theoretical model can be checked with these experiments as well as with those on platinum alloys.[11] Section IV contains a determination of the values of the indirect coupling constants for lead and platinum metals. The data of Sec. III are used together with those obtained from a study of cw lineshape of the pure metals, based on the theory of exchange narrowing.[17] The lead results are discussed in terms of the band structure of this metal.

II. CALCULATION OF THE SPIN-ECHO ENVELOPE

A. Hamiltonian

In a high magnetic field, the principal term in the Hamiltonian for the resonant spins I is the Zeeman term $\mathcal{H}_Z^0=-\omega_0\sum_j I_j^z$, where the $0z$ axis is along the magnetic field H_0 and ω_0 is the central resonance frequency. The distribution of the Knight shift values introduces an additional term $\mathcal{H}_Z^1=-\sum_j \delta\omega_j I_j^z$. The resonance frequency of the spin j is $\omega_j=\omega_0+\delta\omega_j$. In the total Hamiltonian $\mathcal{H}$, only the terms commuting with the principal part $\mathcal{H}_Z^0$ will be taken into account. Thus one has

$$\begin{aligned}\mathcal{H}&=\mathcal{H}_Z^0+\mathcal{H}_Z^1+\mathcal{H}_q+\mathcal{H}_{dd}+\mathcal{H}_{ex}+\mathcal{H}_{IS}+\mathcal{H}_S\\&=\mathcal{H}_Z^0+\mathcal{H}_Z^1+\sum_j a_j(I_j^z)^2+\tfrac{1}{2}\sum_{j,k\neq} B_{jk}(\mathbf{I}_j\cdot\mathbf{I}_k-3I_j^zI_k^z)\\&\quad+\tfrac{1}{2}\sum_{j,k\neq} J_{jk}\mathbf{I}_j\cdot\mathbf{I}_k+\sum_{j,k'} C_{jk'}I_j^zS_{k'}^z+\mathcal{H}_S. \qquad (1)\end{aligned}$$

$\mathcal{H}_q$ represents the quadrupolar couplings, and a_j is defined by

$$a_j=[3eQ/8I(2I-1)\hbar]eq_j(3\cos^2\epsilon_j-1).$$

Here eQ is the quadrupolar moment of the nucleus and eq_j is the electric field gradient which is assumed to have axial symmetry around an axis z_j which makes an angle ϵ_j with the magnetic field H_0. $\mathcal{H}_{dd}$ involves both dipolar and pseudodipolar interactions between spins I. Here

$$B_{jk}=\tfrac{1}{2}(\gamma_I^2\hbar/r_{jk}^3+b_{jk})(3\cos^2\theta_{jk}-1),$$

where r_{jk} is the distance between the jth and kth nuclei and θ_{jk} is the angle between r_{jk} and the $0z$ axis. The radial part of the pseudodipolar interaction is b_{jk}. $\mathcal{H}_{ex}$ is the indirect exchange coupling between the spins I. $\mathcal{H}_{IS}$ represents all interactions between resonant spins I and the nonresonant nuclear spin species. It is also truncated in order to commute with $\mathcal{H}_Z^0$. In this paper only one type of S spin is assumed. This restriction is not important and can easily be removed. $\mathcal{H}_S$ includes the Zeeman, quadrupolar, and spin–spin terms for S spins.

In this Hamiltonian the spin–spin interactions give rise to what will be called a homogeneous broadening of the NMR absorption line. An inhomogeneous broadening is produced when the resonant spins of the sample are coupled with electric field gradients or effective magnetic fields which are not identical. In such a case, the contributions of the jth spin I to $\mathcal{H}_Z^1$ and $\mathcal{H}_q$ vary with the index j. According to this definition,[18] only the terms which are functions of I_j^z alone can contribute to the inhomogeneous broadening. In alloys, such effects can originate from several sources: e.g., the anisotropy of the Knight shift,[19] the demagnetizing fields in the case of a strong paramagnetic susceptibility,[20] or the spatial oscillations of the Knight shift or of the electric field gradients. The last two effects differ from the two others in the sense that they produce inhomogeneities on a microscopic scale. The distinction is essential in the calculation which follows. As the spin–spin interactions decrease as $1/r^3$, one can roughly define a critical radius R_c beyond which these interactions can be neglected. If within this radius the terms of $\mathcal{H}_Z^1$ and $\mathcal{H}_q$ introduce variations bigger than the strength of the spin-spin interactions, the broadening is microscopic or local. Otherwise it is macroscopic.

B. Basic Assumptions of the Model

The temperature is assumed to be low enough so that there is no atomic diffusion in the sample, and the spin lattice relaxation time T_1 is sufficiently long so as not to contribute to the linewidth. Further the intensity of the rf pulses H_1 should be large enough so that the whole NMR spectrum of the spins I can be flipped. This last condition may be difficult to fulfill for spins bigger than $\frac{1}{2}$. In such cases, the distribution of quadrupolar satellites may extend far away from the central line.

The calculation applies to a 90°–180° coherent pulse sequence with a variable time τ between the two pulses. The spin echo occurs at a time 2τ and its intensity is given by

$$E(2\tau)\propto\langle I_x\rangle_{av}\propto \mathrm{Tr}\,\{\rho(2\tau)I_x\}, \qquad (2)$$

with

$$\langle I_y\rangle_{av}=0,$$

where $\rho(2\tau)$ is the density matrix of the whole spin system describing the motion of the spins in the rotating frame, $I_x=\sum_l I_l^x$, and the trace is taken in the space of the spins I and S. Before the first pulse, the spin system is at thermal equilibrium and its den-

[16] R. J. Snodgrass and L. H. Bennett, Phys. Rev. **132**, 1465 (1963).
[17] P. W. Anderson and P. R. Weiss, Rev. Mod. Phys. **25**, 269 (1953).
[18] J. M. Winter, *Quantum Optics and Electronics* (Gordon and Breach Science Publishers, Inc., New York, 1964), p. 570.
[19] N. Bloembergen and T. J. Rowland, Acta Met. **1**, 731 (1953).
[20] L. E. Drain, Proc. Phys. Soc. (London) **80**, 1380 (1962).

sity matrix is

$$\rho(0) \propto \exp(-\hbar\mathcal{H}/kT) \simeq \{1\}+(\hbar\omega_0 I_z+\hbar\omega'_0 S_z)/kT.$$

The term $\{1\}$ and the term involving the Zeeman energy of the S spins $\hbar\omega'_0 S_z=\mathcal{H}_Z{}^S$ do not contribute to the signal because they are not affected by the pulses which act only on the spins I. Thus $\rho(0)$ can be taken as being proportional to I_z. In the rotating frame, the rf pulses correspond to rotations of the coordinate system about the $0y$ axis. Before and after the pulses, the density matrix obeys an equation of motion involving the Hamiltonian $\mathcal{H}'=\mathcal{H}-\mathcal{H}_Z{}^0-(\gamma I/\gamma_S)\mathcal{H}_Z{}^S$. One finds that[21]

$$\rho(2\tau) \propto \exp(-i\mathcal{H}'\tau)\exp(-i\tilde{\mathcal{H}}'\tau)I_x \times \exp(i\tilde{\mathcal{H}}'\tau)\exp(i\mathcal{H}'\tau), \quad (3)$$

where $\tilde{\mathcal{H}}'$ is deduced from $\mathcal{H}'$ by the 180° rotation, and where the $\mathcal{H}_Z{}^S$ terms cancel out. The combination of (2) and (3) gives an expression for the echo envelope $E(2\tau)$ which is impossible to calculate in the general case because the different terms in $\mathcal{H}'$ do not commute.

Case where $\mathcal{H}_{IS}$ can be Neglected

In this situation all the terms involving the spins S disappear in (3). The only term which varies in the passage from $\mathcal{H}'$ to $\tilde{\mathcal{H}}'$ is $\mathcal{H}_Z{}^1$, which changes its sign. This is because the 180° rotation changes $I_j{}^z$ in $-I_j{}^z$ and $I_j{}^x$ in $-I_j{}^x$. Then

$$\mathcal{H}'=\mathcal{H}_Z{}^1+\mathcal{H}_1,$$

and

$$\tilde{\mathcal{H}}'=-\mathcal{H}_Z{}^1+\mathcal{H}_1,$$

where

$$\mathcal{H}_1=\mathcal{H}_q+\mathcal{H}_{dd}+\mathcal{H}_{\rm ex}.$$

Notice at this point that if $\mathcal{H}_Z{}^1$ were to commute with $\mathcal{H}_1$, it would disappear completely from expression (3). This fact is related to the distinction between a macroscopic and a microscopic inhomogeneous term $\mathcal{H}_Z{}^1$.

For a *macroscopic* inhomogeneity, $\mathcal{H}_Z{}^1$ is proportional to $\sum_j I_j{}^z$ in a volume $R_c{}^3$, where R_c was defined by the range of spin-spin interactions. In this volume $[\mathcal{H}_Z{}^1, \mathcal{H}_1]=0$ and the calculation of $E(2\tau)$ leads to the usual result for the echo envelope in pure solids

$$E(2\tau) \propto \mathrm{Tr}\{\exp(-2i\mathcal{H}_1\tau)I_x \exp(2i\mathcal{H}_1\tau)I_x\}. \quad (4)$$

This expression is also true for the whole sample. The magnetic inhomogeneity terms have dropped out while those of quadrupolar origin have been kept. For a spin $I=\frac{1}{2}$, this corresponds to the reduced autocorrelation function which is the Fourier transform of the absorption lineshape.[7]

In the case of alloys, the inhomogeneous broadening occurs at a *microscopic* scale and the above simplification is no longer valid. Assuming the broadening is strong enough, one may have for any pair of spins

$$|\delta\omega_j-\delta\omega_k| \gg b_{jk}, J_{jk}, (\gamma_I{}^2\hbar/r_{jk}{}^3), \quad (5)$$

or

$$|a_j-a_k| \gg b_{jk}, J_{jk}, (\gamma_I{}^2\hbar/r_{jk}{}^3). \quad (5')$$

These conditions mean that the intensity of the spin–spin interactions is weak compared with the variation of the Zeeman or quadrupolar energy. If either is fulfilled, $\mathcal{H}_{\rm ex}$ and $\mathcal{H}_{dd}$ can be taken as perturbations relative to $\mathcal{H}_Z{}^1$ or $\mathcal{H}_q$. In this approximation the terms $I_j{}^x I_k{}^x$ and $I_j{}^y I_k{}^y$ are neglected, as they do not commute with the principal Hamiltonian $\mathcal{H}_Z{}^1$ or $\mathcal{H}_q$. In either cases $\mathcal{H}_Z{}^1$ is again eliminated from expression (3). Thus one has

$$E(2\tau) \propto \mathrm{Tr}\{\exp(-2i\mathcal{H}_1''\tau)I_x \exp(2i\mathcal{H}_1''\tau)I_x\}, \quad (6)$$

with the truncated Hamiltonian

$$\mathcal{H}_1''=\tfrac{1}{2}\sum_{j,k\neq}[J_{jk}-((\gamma_I{}^2\hbar/r_{jk}{}^3)+b_{jk})(3\cos^2\theta_{jk}-1)]I_j{}^z I_k{}^z + \sum_j a_j(I_j{}^z)^2 = \tfrac{1}{2}\sum_{j,k\neq}\tilde{J}_{jk}I_j{}^z I_k{}^z+\sum_j a_j(I_j{}^z)^2. \quad (7)$$

Here the bracket is simply designated by $\tilde{J}_{jk}$. In Sec. II C the calculation of this final expression will be carried out.

General Case where $\mathcal{H}_{IS}$ cannot be Neglected

Here, difficulty arises from the fact that $\mathcal{H}_{IS}$ does not commute with $\mathcal{H}_{dd}$, $\mathcal{H}_{\rm ex}$, or $\mathcal{H}_S$. In this situation a completely different approach has been put forward.[12,22] The spin–spin interactions are represented by fluctuating local fields. The influence of the spins S on the spin-echo envelope of spins I then depends upon the relaxation rate R of the local fields due to the spins S. If $R\tau \gg 1$, these fluctuating fields are nearly averaged out. There is only a small effect of the spins S on the spin-echo envelope and on the free precession decay. It is essentially a case of "motional narrowing." If, on the contrary, the spins S relax very slowly ($R=0$), the local fields are nearly time-independent and they act in the same way as an inhomogeneous Zeeman term. The cases of interest are intermediate. $\mathcal{H}_{IS}$ interactions act partly as inhomogeneities. This explains the existence of solid echoes.[23] Such echoes are observed in solid xenon in an homogeneous external field for a 90°–180° sequence.[24] Another similar example is given by metallic silver.[25] In this case, the spin-echo envelope of a given species decays more slowly than does the

[21] A. Abragam, *The Principles of Nuclear Magnetism* (Clarendon Press, Oxford, England, 1961), p. 499.

[22] M. Emshwiller, E. L. Hahn, and D. Kaplan, Phys. Rev. **118**, 414 (1960).

[23] P. Mansfield, Phys. Rev. **137**, A961 (1965).

[24] W. W. Warren, Jr., and R. E. Norberg, Phys. Rev. **154**, 277 (1967).

[25] A. Narath, A. T. Fromhold, Jr., and E. D. Jones, Phys. Rev. **144**, 428 (1966).

free precession in a homogeneous field. However, the decay is faster than what is calculated on the basis of interactions between like spins only. Thus for alloys one should expect that the coupling between unlike spins will produce a damping of the spin-echo envelope given by expression (6). The latter will now be calculated.

C. The Separation of Quadrupolar and Spin-Spin Interactions in $E(2\tau)$

In this calculation, no attention will be paid to constant factors which can be taken out of the trace operation. At the end, the multiplicative constant will be determined by the condition $E(0)=1$. From (8) and (7) one has

$$E(2\tau) \propto \mathrm{Tr}\{\exp[-i\tau \sum_{j,k\neq} \tilde{J}_{jk} I_j^z I_k^z]$$
$$\times \exp[-2i\tau \sum_m a_m (I_m^z)^2] \sum_l I_l^x \exp[2i\tau \sum_m a_m (I_m^z)^2]$$
$$\times \exp[i\tau \sum_{j,k\neq} \tilde{J}_{jk} I_j^z I_k^z] \sum_p I_p^x\}.$$

As $[I_m^z, I_l^x]=0$ for $m\neq l$, all the terms with $m\neq l$ disappear from this expression. The same thing happens to the terms which have both $j\neq l$ and $k\neq l$. Consequently, one obtains

$$E(2\tau) \propto \mathrm{Tr}\{\sum_l \exp[-2i\tau \sum_{j\neq l} \tilde{J}_{jl} I_j^z I_l^z]$$
$$\times \exp[-2i\tau \sum_l a_l (I_l^z)^2] I_l^x \exp[2i\tau \sum_l a_l (I_l^z)^2]$$
$$\times \exp[2i\tau \sum_{j\neq l} \tilde{J}_{jl} I_j^z I_l^z] \sum_p I_p^x\}.$$

Defining $\Gamma_l \equiv 2\tau \sum_{j\neq l} \tilde{J}_{jl}$ and $\alpha_l \equiv 2\tau a_l$, one may write

$$E(2\tau) \propto \mathrm{Tr}\{\sum_l \exp[-i\alpha_l (I_l^z)^2] \exp[-i\Gamma_l I_l^z] I_l^x$$
$$\times \exp[i\Gamma_l I_l^z] \exp[i\alpha_l (I_l^z)^2] \sum_p I_p^x\}$$
$$\propto \mathrm{Tr}\{\sum_l \exp[-i\alpha_l (I_l^z)^2][I_l^x \cos\Gamma_l + I_l^y$$
$$\times \sin\Gamma_l] \exp[i\alpha_l (I_l^z)^2] \sum_p I_p^x\}.$$

Here $\exp(-i\Gamma_l I_l^z)$ has been treated as a rotation operator acting on I_l^x, since Γ_l is independent of the spin I_l. For this reason one can also write

$$E(2\tau) \propto \sum_{l,p} \mathrm{Tr}\{A_l^x \cos\Gamma_l I_p^x + A_l^y \sin\Gamma_l I_p^x\},$$

where

$$A_l^x = \exp[-i\alpha_l (I_l^z)^2] I_l^x \exp[i\alpha_l (I_l^z)^2],$$
$$A_l^y = \exp[-i\alpha_l (I_l^z)^2] I_l^y \exp[i\alpha_l (I_l^z)^2].$$

In the last summation, the l spin is only found in the A_l^x and A_l^y operators for terms with $p\neq l$. Thus the trace factors in the following way:

$$\mathrm{Tr}\{A_l^x \cos\Gamma_l I_p^x\} = \mathrm{Tr}_l\{A_l^x\} \mathrm{Tr}_{j\neq l}\{\cos\Gamma_l I_p^x\},$$

where $\mathrm{Tr}_{l,\cdots,n}$ indicates that the trace is taken over a complete space of eigenfunctions of $I_l, \cdots, I_n$. Since $\mathrm{Tr}_l\{A_l^x\} = \mathrm{Tr}_l\{I_l^x\} = 0$, one finds that the terms containing A_l^x disappear from the summation for $l\neq p$. This is also true for the term in A_l^y. Thus one ends up with a simple summation

$$E(2\tau) \propto \sum_l [\mathrm{Tr}\{A_l^x \cos\Gamma_l I_l^x\} + \mathrm{Tr}\{A_l^y \sin\Gamma_l I_l^x\}]$$
$$\propto \sum_l [\mathrm{Tr}_l\{A_l^x I_l^x\} \mathrm{Tr}_{j\neq l}\{\cos\Gamma_l\}$$
$$+ \mathrm{Tr}_l\{A_l^y I_l^x\} \mathrm{Tr}_{j\neq l}\{\sin\Gamma_l\}].$$

Now one must calculate $\mathrm{Tr}_{j\neq l}\{\cos\Gamma_l\}$ and $\mathrm{Tr}_{j\neq l}\{\sin\Gamma_l\}$. For this calculation one introduces $\gamma_{jl} = 2\tau \tilde{J}_{jl}$, so that

$$\cos\Gamma_l = \cos(\sum_{j\neq l} \gamma_{jl} I_j^z)$$
$$= \tfrac{1}{2} \prod_{j\neq l} \exp(i\gamma_{jl} I_j^z) + \tfrac{1}{2} \prod_{j\neq l} \exp(-i\gamma_{jl} I_j^z),$$
$$\sin\Gamma_l = \sin(\sum_{j\neq l} \gamma_{jl} I_j^z)$$
$$= (2i)^{-1} \prod_{j\neq l} \exp(i\gamma_{jl} I_j^z) - (1/2i) \prod_{j\neq l}$$
$$\times \exp(-i\gamma_{jl} I_j^z).$$

Also

$$\mathrm{Tr}\{\prod_{j\neq l} \exp(i\gamma_{jl} I_j^z)\} = \prod_{j\neq l} \mathrm{Tr}_j\{\exp(i\gamma_{jl} I_j^z)\}$$
$$= \prod_{j\neq l} \sum_{m=-I}^{+I} \exp(im\gamma_{jl})$$
$$= \mathrm{Tr}\{\prod_{j\neq l} \exp(-i\gamma_{jl} I_j^z)\},$$

$$\mathrm{Tr}\{\cos\Gamma_l\} = \prod_{j\neq l} \sum_{m=-I}^{+I} \exp(im\gamma_{jl}),$$

$$\mathrm{Tr}\{\sin\Gamma_l\} = 0.$$

This simplifies the expression of the echo amplitude, which becomes

$$E(2\tau) \propto \sum_l \mathrm{Tr}_l\{\exp[-i\alpha_l (I_l^z)^2] I_l^x \exp[i\alpha_l (I_l^z)^2] I_l^x\}$$
$$\times \prod_{j\neq l} \sum_{m=-I}^{+I} \exp(im\gamma_{jl}),$$

where one remembers that the parameters γ_{jl} and α_l are related to the coupling constants by

$$\gamma_{jl} \equiv 2\tau \tilde{J}_{jl}$$
$$\equiv 2\tau\{J_{jl} - [(\gamma_I^2 \hbar / r_{jl}^3) + b_{jl}) (3\cos^2\theta_{jl} - 1]\},$$
$$\alpha_l \equiv 2\tau a_l$$
$$\equiv 2\tau [3eQ/8I(2I-1)\hbar] e q_l (3\cos^2\epsilon_l - 1). \quad (8)$$

Thus in the expression for $E(2\tau)$, two factors appear under the sign $\sum_l$: The first involves the intensity and orientation of the electric field gradient at the

site l only, while the second is characterized by the spin-spin interactions with a given configuration of the neighboring spins I. As the resonating spin system contains a large number N of spins, the sites with a given configuration of the neighboring spins can be submitted to various electric field gradients defined by q and ϵ. One may assume that the distribution of q and ϵ is the same for all possible spin configurations. This approximation is good for a strong isotopic dilution of the spins I, as well as for high concentration alloys. As a consequence of this, $E(2\tau)$ splits into two factors

$$E(2\tau)=E_1(2\tau)\times E_2(2\tau), \tag{9}$$

with

$$E_1(2\tau)=C_1^{-1}\iint \mathrm{Tr}_l\{\exp[-2ia\tau(I_l^z)^2]I_l^x \times \exp[2ia\tau(I_l^z)^2]I_l^x\}f(q,\epsilon)\sin\epsilon\, dqd\epsilon, \tag{10}$$

where $f(q, \epsilon)$ is the distribution function of the electric field gradients normalized to unity, and

$$E_2(2\tau)=C_2^{-1}\sum_{\lambda}\prod_{j\neq 0}\sum_{m=-I}^{+I}\exp(2i\tau m\tilde{J}_{j0}), \tag{11}$$

where the summation over λ is a summation over all possible spin configurations around the central spin with index 0. Both C_1 and C_2 can be determined by putting $E_1(0)=E_2(0)=1$.

D. Quadrupolar Effects on the Spin-Echo Envelope

$E_1(2\tau)$, given by (10), describes the quadrupolar effects on the spin-echo envelope. The same expression follows directly from (4) if the spin–spin interactions are neglected, i.e., by putting $\mathcal{H}_1=\mathcal{H}_Q$. In the case of a unique field gradient of intensity q_0 and orientation ϵ_0, the function $E_1(2\tau)$ is periodic, its frequency depending upon the parameter $a_l=a_0$ as defined by (8). This effect has been observed in ferromagnetic compounds[14] and cobalt.[26] In a disordered nonmagnetic alloy, the distribution of electric field gradients is very wide, and experimentally it turns out to be difficult—if not impossible—to make the rf pulse big enough to flip the whole spectrum. In the cases where the difficulty could be overcome. The $E_1(2\tau)$ term should only introduce a damping of the spin-echo envelope.

Finally, it should be mentioned that the multiple quadrupolar echoes of Solomon[13] cannot be observed in alloys with a large enough magnetic inhomogeneous broadening.[15] The only echo which occurs is the one we have calculated for the time 2τ. No further discussion of quadrupolar effects will be given as these have been extensively discussed in the above references. The important point of the calculation of Sec. II C is that these effects appear separately in the expression for $E(2\tau)$.

[26] P. C. Riedi and R. G. Scurlock, Phys. Letters **24A**, 42 (1967).

E. Effect of the Spin-Spin Interactions on the Spin-Echo Envelope

The computation can be restricted to the first-nearest neighbors, as the spin-spin interactions decrease as $1/r^3$. Thus one has

$$J_{j0}=J,$$

$$b_{j0}=b,$$

$$r_{j0}=d,$$

when j represents a first-nearest neighbor of the central spin 0 and $\tilde{J}_{j0}=0$ otherwise. Thus for first-nearest neighbors

$$\tilde{J}_{j0}=J-B(3\cos^2\theta_{j0}-1),$$

where $B=\gamma_I^2\hbar/d^3+b$. The effect of more distant neighbors will be studied at the end of this chapter.

An integration over angular dependence of formula (11) must be carried out. The spins having the same configuration of first-neighbors spins I form a group with a contribution to the echo envelope which can be evaluated separately. The spins I having a concentration c are supposed to be randomly distributed on the lattice sites. The probability for a spin I to be surrounded by r like neighbors is

$$P_r=\binom{r_0}{r}c^r(1-c)^{r_0-r},$$

where r_0 is the total number of next-nearest neighbors ($r_0=12$ for a fcc lattice), and $\binom{r_0}{r}$ is the binomial coefficient. For a given value of r, there are n_r geometrical configurations $C_{n,r}$ with a weight factor $\rho_{n,r}$ normalized to

$$\sum_{n=1}^{n_r}\rho_{n,r}=1.$$

If **i**, **j**, **k** is a frame of reference defined by the lattice the r sites of the $C_{n,r}$ configuration are in positions de-

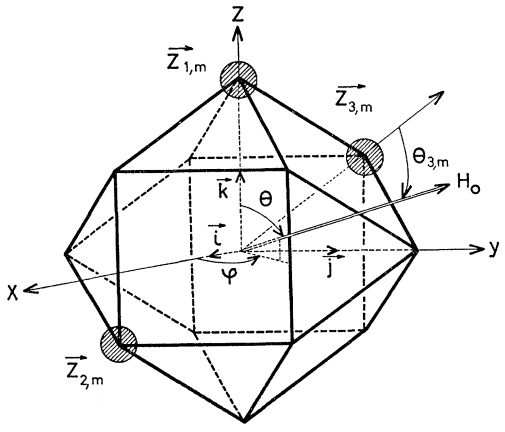

FIG. 1. Dodecahedron of the first-nearest neighbors in a fcc lattice. A configuration $C_{m,3}$ of three spins around the central spin 0 is represented as an example.

fined by the unit vectors:

$$\mathbf{Z}_{\alpha,n}=a_{\alpha,n}\mathbf{i}+b_{\alpha,n}\mathbf{j}+c_{\alpha,n}\mathbf{k}, \qquad (\alpha=1, \cdots, r).$$

Such a configuration is illustrated in Fig. 1. The total contribution $E_{n,r}(2\tau)$ to the echo envelope of the central spins of a configuration $C_{n,r}$ is derived from an integration over the angular orientation of the **i**, **j**, **k** frame relative to the magnetic field. This is identical to a fixed frame of reference and an integration over all orientations (θ, ϕ) of the magnetic field. The angle $\theta_{\alpha,n}$ of $\mathbf{Z}_{\alpha,n}$ with $\mathbf{H}_0$ is given by

$$\theta_{\alpha,n}=\mathbf{Z}_{\alpha,n}\cdot\mathbf{H}_0/H_0$$
$$=a_{\alpha,n}\sin\theta\cos\phi+b_{\alpha,n}\sin\theta\sin\phi+c_{\alpha,n}\cos\theta.$$

This is the angle which appears in the dipolar coupling between the central spin and its first neighbor in the direction $\mathbf{Z}_{\alpha,n}$. The contribution of all central spins

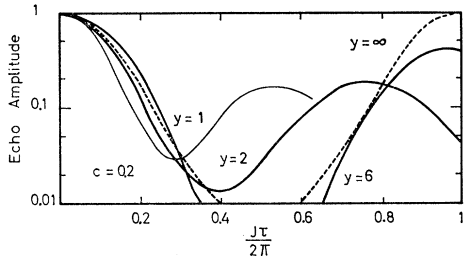

FIG. 2. Calculated echo envelopes for various values of the parameter $y=J/B$ and for a concentration $c=0.2$ of the resonant spins $I=\frac{1}{2}$. These curves show how the dipolar interaction affects the modulation frequency and introduces a damping.

of the same group may thus be written as

$$E_{n,r}(2\tau)=\frac{1}{4\pi(2I+1)^r}\iint\prod_{n=1}^{r}\sum_{m=-I}^{+I}$$
$$\times\exp[2i\tau m(J+B-3B\cos^2\theta_{\alpha m})]\sin\theta d\theta d\phi. \quad (12)$$

Finally $E_2(2\tau)$ is the sum of all contributions of the above form[12]

$$E_2(2\tau)=\sum_{r=0}^{r_0}P_r\sum_{n=1}^{n_r}\rho_{n,r}E_{n,r}(2\tau). \quad (13)$$

This formula is the general result for the contribution to the echo envelope of the spin-spin interactions between first-nearest neighbors only. Three distinct cases can be analyzed, depending upon the strength of the indirect exchange coupling relative to the dipolar couplings.

Case Where $J\gg B$

In such a limiting case the angular dependence disappears and one has

$$E_2(2\tau)=\sum_{r=0}^{r_0}P_r\frac{1}{(2I+1)^r}\sum_{m=-I}^{+I}\exp(2im\tau J). \quad (14)$$

For $I=\frac{1}{2}$, this formula reduces to the earlier results[11]:

$$E_2(2\tau)=\sum_{r=0}^{r_0}P_r\cos^r(J\tau).$$

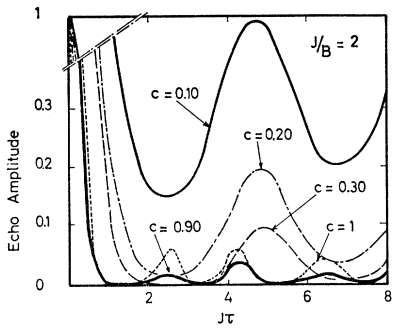

FIG. 3. Calculated echo envelopes for various concentrations c of the resonant spins $I=\frac{1}{2}$, and for a fixed value $J/B=2$. The modulation frequency has only a slight dependence upon c, except for a frequency doubling phenomenon occurring near $c=1$. The damping increases strongly with c, however.

For any spin value the echo envelope is a periodic function. One may easily deduce from (14) that the period is π/J for integer values of I and $2\pi/J$ for half integer values of I. $E_2(2\tau)$ is always positive and its value oscillates between 1 and a very small minimum. For a large value of I, $E_2(2\tau)$ appears as a succession of spikes at the times $n\pi/J$ for integer values of I, and at $2n\pi/J$ for half-integer values. When I is a half integer, the proportion of second harmonic becomes important as the concentration c of the spins I increases. Thus the period is divided by a factor of 2 when c approaches unity.

Case Where J and B Are About Equal

In this case $E_{m,r}(2\tau)$ must be computed. This has been done for $I=\frac{1}{2}$. The results, illustrated in Fig. 2 for a given value of c, exhibit damped modulations at a frequency depending upon the parameter $y=J/B$. This frequency decreases when B decreases, its lower limit being $J/2\pi$. It varies only very slightly with c, as is shown on Figs. 3 and 4. The frequency doubling for $c\simeq 1$ occurs here as well as in the preceding case.

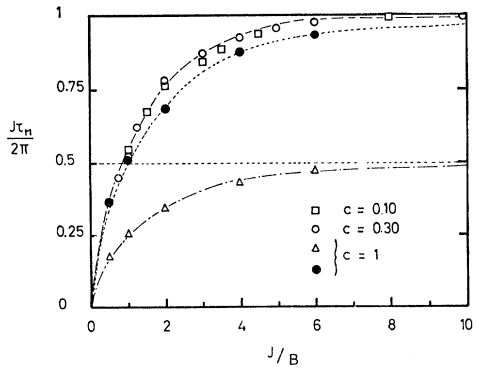

FIG. 4. Calculated value of the echo envelope modulation period $2\tau_M$, in units of $4\pi/J$ versus the parameter J/B for three different concentrations c and $I=\frac{1}{2}$. For $c=1$, a double curve has been plotted: one at the true period and one at twice this value. The latter does not depart very much from the curve drawn through the points corresponding to small c values.

Pure Dipolar Case $J=0$

Here the calculated echo envelopes do not present noticeable features in the preceding case. The envelopes oscillate very slightly with an amplitude which is too small to be significant when compared with the influence of further neighbors. The decay time of the echo envelope T_2 is expected to be larger in the alloy than in the pure metal in the case $J=0$. This is due to the decoupling of the spins by the local inhomogeneity, which inhibits the influence of the flip-flop terms $I_j^+ I_k^-$.

Interactions with the Second-Nearest and Further Neighbors

The general expression (11), with the spin-spin interactions restricted to first- and second-nearest-neighbor interactions only, can be written as

$$E_2(2\tau) \propto \sum_{\lambda} \prod_{j} \left[\sum_{m=-I}^{+I} \exp(2im\tau \tilde{J}_{j0}) \right] \prod_{k} \times \left[\sum_{m=-I}^{+I} \exp(2im\tau \tilde{J}_{k0}) \right].$$

Here j and k are product indices over the first and second neighbors, respectively. The λ summation is taken over all possible configurations of the first- and second-nearest neighbors. These two types of configurations being uncorrelated, the expression factors into the product of two distinct summations

$$E_2(2\tau) \propto \left\{ \sum_{\lambda_1} \prod_{j} \left[\sum_{m=-I}^{+I} \exp(2i\tau m \tilde{J}_{j0}) \right] \right\} \times \left\{ \sum_{\lambda_2} \prod_{k} \left[\sum_{m=-I}^{+I} \exp(2i\tau m \tilde{J}_{k0}) \right] \right\}. \quad (15)$$

The first bracket of (15) is the starting formula for first-neighbor couplings only. The interactions with the second neighbors appear similarly in the second bracket. The latter factor, represents a superimposed modulation characterized by the couplings with the second-nearest neighbors. The frequency of this modulation is generally expected to be smaller than that due to the first neighbors. This result can easily be extended to further groups of neighbors. Experimentally, however, it is likely that only the highest modulation frequency will be observable.

In conclusion, it turns out that quadrupolar and spin–spin interactions have distinct influences on the shape of spin-echo envelopes, assuming that the local inhomogeneous broadening is strong enough. In particular, the exchange coupling produces a modulation of the spin-echo envelope. The frequency of this modulation has been related to the spin–spin coupling constants J and B.

III. EXPERIMENTAL RESULTS

The experiments have been performed in various lead alloys. Lead was chosen as a solvent for several reasons. First, it has only one isotope with nonzero spin: Pb^{207} ($I=\frac{1}{2}$), with a natural abundance of 21%. Second, in the pure metal the strength of both exchange and pseudodipolar indirect spin-spin couplings were thought to be about equal and one order-of-magnitude stronger than the ordinary dipolar interaction. Third, the Knight shift is large; 1.47%. Thus strong inhomogeneous broadening occurs in the solid solutions[16] which lead forms with many other metals. In all the experiments described below, the NMR was performed on Pb^{207} at liquid-helium temperature. The external magnetic field was varied between 10 and 14 kG so that the samples were always in the nonsuperconducting state.

A. Samples

The samples were powdered solid solutions of In, Hg, Tl, and Bi in lead. The constitutents were 99.999% pure. The powders were obtained by filing the ingots. Optical spectrography showed that this method introduced no ferromagnetic impurities in the samples. The particles were regularly shaped, of maximum diameter ($2t$) less than 40 μ. The skin depth δ for the samples studied was always bigger than 30 μ for a frequency of 10 MHz at liquid-helium temperature. Thus the ratio $2t/\delta$ was always smaller than 1 so that the penetration of the rf field was practically complete and there was almost no distortion of the NMR lineshape. This was not true for the pure lead sample obtained by chemical means with a particle size less than 5μ. In this case, the residual resistivity was very low and $2t/\delta$ was of the order of 3. The effect on the cw lineshape for this case will be studied in more detail in Sec. IV.

B. Spin-Echo Experiments

In the alloys under study, the inhomogeneous width was usually big enough so that spin echoes were observable in a homogeneous external magnetic field. The echo width was of the order of 20 to 40 μsec, which was several times longer than the duration of the applied pulse for which the rotating rf field H_1 was between 50 and 90 G. The pulse sequences were 90°–180° with the two pulses separated by a variable time τ. The free precession decay signals were not always observed, since the dead time of the spectrometer receiver was about 15 μsec. The technique used in recording the spin-echo envelope has been improved over that reported previously.[27] The signal-to-noise ratio was increased by means of a boxcar integrator. The input to the boxcar was taken from the receiver output, gated so as to present the maximum of the echo amplitude.

[27] H. Alloul and C. Froidevaux, XIVth *Colloque Ampère Ljubljana 1966* (North-Holland Publishing Company, Amsterdam 1966).

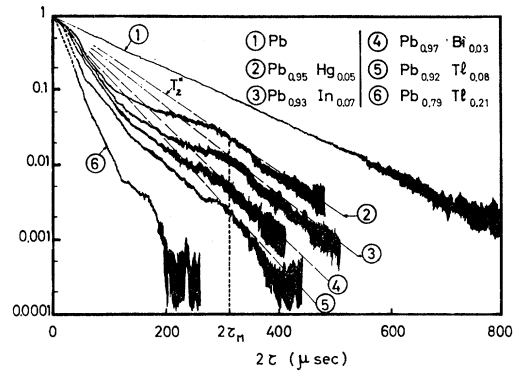

FIG. 5. Experimental spin-echo envelopes of Pb^{207} for different types of alloys taken at 1.4°K in a magnetic field of 13.6 kG. The modulation frequency is independent of the nature of the solute. This is in contrast to the variation of the over-all decay time T_2^* from one sample to the next.

The gate was maintained at time 2τ after the initiation of the 90°–180° transmitter sequence by a circuit similar to that described by Clark.[28] The data were read out on an X-Y recorder: The boxcar output was fed through a logarithmic converter to the Y axis input of the recorder, and a voltage proportional to the pulse spacing 2τ was used to drive the X axis input. The resulting curves shown in Fig. 5 and 6, are of the echo amplitude on a logarithmic scale, plotted versus 2τ.

The spin-echo envelopes all exhibited a modulation, except for two cases: $Pb_{0.79}$–$Tl_{0.21}$, for which the envelope decayed too abruptly and pure lead, for which the envelope is exponential. The important experimental features were that the period of the modulation was independent of the temperature (from 1.2 to 4.2°K), the magnetic field, the nature of the solute and its concentration. Within experimental error the value of this period was found to be $2\tau_M = 305 \pm 15$ μsec. These observations indicate that this value of the period is directly related to the physical properties

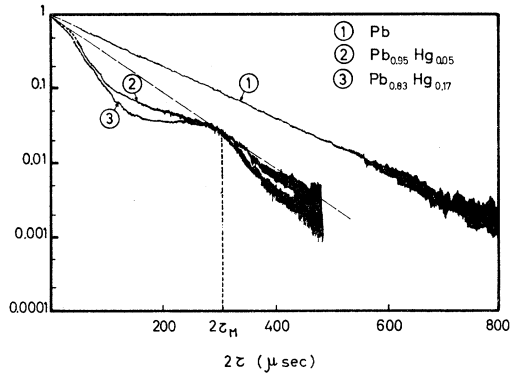

FIG. 6. Experimental spin-echo envelopes of Pb^{207} for two different concentrations of mercury of the alloy at 1.4°K in a magnetic field of 13.6 kG. The amplitude of the modulation varies strongly, whereas its frequency and the over-all decay time T_2^* remain unchanged.

[28] W. G. Clark, Rev. Sci. Instr. **35**, 316 (1964).

TABLE I. Intensity of the couplings between the resonant spins I and nonresonant spins S in two platinum alloys. The peak-to-peak width ΔH of the derivative of the absorption line has been measured in an external field of 14 kG at 1.2°K. The accuracy is 10%. The parameters $\mathfrak{D}$ and $\mathfrak{E}$ are defined in the text. The calculation of $\mathfrak{E}$ is based upon the values of the hyperfine structure constants derived from optical spectra.

Alloy	ΔH (gauss)	$\mathfrak{D}$	$\mathfrak{E}$
$Pt_{0.94}$–$Au_{0.06}$	90	0.065	0.12
$Pt_{0.9}$–$Ir_{0.1}$	100	0.09	0.12

of the pure metal matrix. However the over-all decay time T_2^* of the echo envelope varies from one sample to the next as is shown in Fig. 5. Furthermore, the amplitude of the modulation increases with the concentration of the solute. This is pictured on Fig. 6. These experimental facts will be explained on the basis of the above theoretical model. The same treatment will be applied to the earlier experiments[11] carried out on platinum alloys.

C. Comparison between Theory and Experiments

Both Pb^{207} and Pt^{195} have a spin $\frac{1}{2}$, so that there are no quadrupolar effects. The first condition for the validity of the above calculation is given by (5). It requires a strong local inhomogeneous broadening. Very crudely, this means that the absorption linewidth must be at least an order-of-magnitude bigger in the alloy than in the pure metal. The relevant data are given on the first line of Tables I and II. A second hypothesis of the calculation is that the interactions with the nonresonant spins be smaller than the interaction between I spins. To check this, an estimation of the relative importance of the spin-spin interactions between I and S spins as compared to those between I spins is necessary. For the pure dipolar part one considers the

TABLE II. Intensity of the couplings between the resonant spins I and nonresonant spins S in various lead alloys. The peak-to-peak width ΔH of the derivative of the absorption line has been measured in an external field of 14 kG at 1.2°K. The accuracy is 10%. The parameters $\mathfrak{D}$ and $\mathfrak{E}$ are defined in the text. The calculation of $\mathfrak{E}$ is based upon the values of the hyperfine structure constants derived from optical spectra. The experimental over-all decay time T_2^* is determined as in Fig. 5.

Alloy	ΔH (gauss)	$\mathfrak{D}$	$\mathfrak{E}$	T_2^* (μsec)
$Pb_{0.95}$–$Hg_{0.05}$	30	0.2	0.9	83
$Pb_{0.83}$–$Hg_{0.17}$	65	0.36	1.65	83
$Pb_{0.93}$–$Jn_{0.07}$	30	2.4	0.44	70
$Pb_{0.97}$–$Bi_{0.03}$	16	1.15	1.8	62
$Pb_{0.92}$–$Tl_{0.08}$	25	1.15	2.3	51
$Pb_{0.79}$–$Tl_{0.21}$	43	1.85	3.7	~32

ratio of the respective contributions to the second moment

$$\mathfrak{D}^2=\Delta\omega_{IS}^2/\Delta\omega_{II}^2$$
$$=\frac{4}{9}\left(\frac{\gamma_S}{\gamma_I}\right)^2\frac{c_S}{c_I}\frac{S(S+1)}{I(I+1)},$$

where γ_S, γ_I, c_S, and c_I are, respectively, the gyromagnetic ratios and the concentrations of the spins S and I. For the exchange interaction, one can define an analogous parameter

$$\mathcal{E}^2=\frac{c_S}{c_I}\frac{S(S+1)}{I(I+1)}\left(\frac{J_{IS}}{J_{II}}\right)^2,$$

where J_{IS} and J_{II} are the Ruderman-Kittel coupling constants between first-nearest neighbors.

From

$$\hbar J_{ij}=\frac{\Omega^2 m^*\xi_i\xi_j a_i(s)\,a_j(s)}{4(2\pi)^3\hbar^2 r_{ij}^4}$$
$$\times[2k_F r_{ij}\cos(2k_F r_{ij})-\sin(2k_F r_{ij})], \quad (16)$$

where

$$\xi_i=\langle|\psi_i(0)|^2\rangle/\phi_i^2(0),$$

and

$$\xi_j=\langle|\psi_j(0)|^2\rangle/\phi_j^2(0)$$

are the ratios between the electronic density at the nucleus in the alloy and in a s state of the free atom, and where $a_i(s)$ and $a_j(s)$ are the hyperfine structure constants. In this last expression, Ω is the volume of the atomic cell, m^* the effective mass of the electrons, k_F the wave vector at the Fermi level, and r_{ij} the distance between the ith and jth spins. It follows immediately that

$$\frac{J_{IS}}{J_{II}}=\frac{\xi_S}{\xi_I}\frac{a_S(s)}{a_I(s)},$$

where the subscripts refer to the spin species I and S. The values of $\mathcal{E}$ given in Table I are based on the commonly made assumption[29,30] that $\xi_S=\xi_I$. Thus

$$\mathcal{E}^2=\frac{c_S}{c_I}\frac{S(S+1)}{I(I+1)}\left[\frac{a_S(s)}{a_I(s)}\right]^2.$$

One assumes that the results for the pseudodipolar couplings will not differ considerably from those illustrated by $\mathfrak{D}$ and $\mathcal{E}$.

From Tables I and II, it is clear that the assumptions of the theoretical model are much better fulfilled in the platinum than in the lead alloys. In the platinum case, the interactions with the nonresonant spins are truly negligible, and the observed linewidth is much bigger than the contribution of spin-spin interactions which can only be of the order of a few G. In the case of lead, the total Knight shift being smaller than in platinum, the inhomogeneous broadening is less important. Furthermore, the $\mathcal{H}_{IS}$ couplings are relatively strong and do affect the echo envelopes according to expectations. Thus the bigger the values of $\mathfrak{D}$ and $\mathcal{E}$, the more the over-all decay time T_2^* departs from the value of T_2 in pure lead. However, this effect is of moderate magnitude and has been shown on Fig. 5 not to modify the modulation frequency. On the other hand, the increasing amplitude of the modulation, shown in Fig. 6, illustrates a case where the effect of the $\mathcal{H}_{IS}$ terms remains small but where the inhomogeneous broadening increases strongly with the concentration. Thus the conditions of the model are more nearly fulfilled for the $Pb_{0.83}$–$Hg_{0.17}$ samples than for the other lead alloys.

So far, all the qualitative features of the experimental echo envelopes have been found to be in agreement with the theory. A quantitative comparison is presented in Fig. 7 for a platinum alloy. The agreement is satisfactory. The fact that the theoretical damping is too weak is related to the absence of the interactions with spins outside the first-nearest neighbors' shell in the theoretical model used in the computation. Formula (15) predicts such an additional damping. Finally, one should notice that although the linewidth is large, the condition for *local inhomogeneous broadening* is surely not fulfilled for all pairs of spins. Thus some spins may give rise to an unmodulated contribution to the echo envelope. This raises the value of the total echo at the minima of the echo envelope. This effect is particularly marked in the lead alloys, but it is seen to be quite small in the case of platinum alloys, illustrated in Fig. 7. There, less than 10% of the signal strength appears to be unmodulated.

The most important quantitative experimental results are the measured modulation frequencies of the

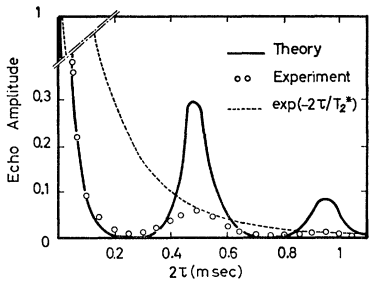

FIG. 7. Comparison between the experimental spin-echo envelope of Pt^{195} in a $Pt_{0.94}$–$Au_{0.06}$ sample and a theoretical curve. The latter is based on a model where only the spin-spin interactions between first-nearest neighbors are taken into account. It implies a value of B for the parameter J/B in agreement with the results presented in Sec. IV.

[29] W. D. Knight, in *Solid State Physics*, edited by F. Seitz and D. Turnbull (Academic Press Inc., New York, 1956) Vol. 2, p. 93.

[30] E. Daniel, J. Phys. Chem. Solids **10**, 174 (1959).

echo envelopes. They will make it possible to determine the strength of the indirect spin–spin couplings.

IV. THE INDIRECT SPIN-SPIN COUPLING CONSTANTS IN LEAD AND PLATINUM METALS

The results of the calculation presented in Part II yield a relationship between the modulation period $2\tau_M$, J, and B. In order to determine separately the coupling constants J and B, one has to use a second relationship derived from the observation of the cw lineshape in the pure metals.

A. Exchange Narrowing in the Pure Metal

The natural isotopic abundance of Pb^{207} and Pt^{195} are $c=0.21$ and $c=0.33$, respectively. In such cases, and in the presence of pure dipolar couplings only, one would expect the absorption lineshape to be Gaussian.[31] The fact that in both lead and platinum the experimental lines are Lorentzian is connected with a strong exchange interaction between like spins. This increases the value of the fourth moment of the absorption line without modifying the second moment. The half intensity linewidth $2\delta\omega$ has been calculated by Anderson and Weiss[17] for the case $J/B>1$

$$\delta\omega=2\pi\delta\nu=\omega_p^2/\omega_e, \tag{17}$$

where ω_p and ω_e are defined by the expression of the second and fourth moments

$$\langle\Delta\omega^2\rangle=\omega_p^2,$$
$$\langle\Delta\omega^4\rangle=\omega_p^4+(\pi/2)\omega_p^2\omega_e^2.$$

The second moment is given by

$$\omega_p^2=\tfrac{1}{3}I(I+1)c\sum_k B'^2_{jk},$$

where B'_{jk} differs from the above parameter B_{jk} only by a numerical factor $B'_{jk}=-3B_{jk}$. If one makes the assumption than b_{jk} varies as $1/r_{jk}^3$, one has

$$\omega_p^2=\tfrac{3}{5}cI(I+1)B^2\sum_k (d/r_{jk})^6,$$

where d is the distance between first nearest neighbors. For an fcc lattice and a spin $I=\frac{1}{2}$, this becomes

$$\omega_p^2=6.5cB^2. \tag{18}$$

The fourth-moment calculation was carried out[32] for the case where only the first neighbor interactions are taken into account. It leads to

$$\tfrac{1}{2}\pi\omega_p^2\omega_e^2=77.5J^2B^2c^2. \tag{19}$$

Combining (17), (18), and (19), one finds the required second relationship between J and B

$$\delta\omega=2.36(B^2/J)\sqrt{c}. \tag{20}$$

Thus a measurement of $\delta\omega$ is necessary. Formula (18) indicates that a measurement of the second-moment absorption line could yield the value of B. This method however, is extremely inaccurate because of the strong contribution of the wings to the second moment.

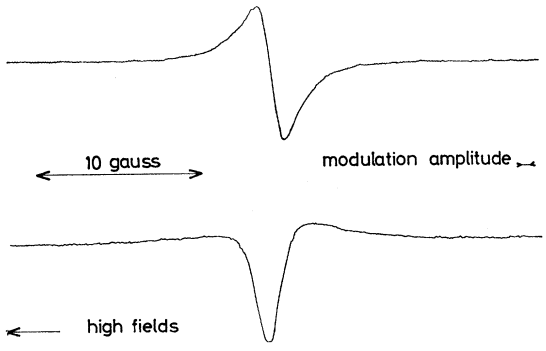

FIG. 8. Experimental in- and out-of-phase NMR signals of Pb^{207} in a powder of pure lead. The particles are roughly spherical with a diameter of about 5 μ. The magnetic field is 5 kG and the temperature 1.2°K.

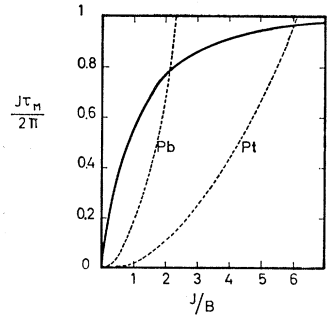

FIG. 9. Graphical detereination of both coupling constants J and B for lead and platinum. The parabolas are based on formula (21) using the experimental modulation period $2\tau_M$ and absorption line halfintensity width $2\delta\nu$ given in Table III.

B. The NMR Lineshape in Pure Lead Metal

The pure lead sample has been studied at 1.2°K with a cross-coil spectrometer having its measuring head in the liquid-helium bath. Both the in-phase and out-of-phase signals $\chi_2(\omega)$ and $\chi_1(\omega)$, respectively, departed slightly from their usual symmetric shapes (Fig. 8). This is due to the fact that the skin depth is smaller than the size of the metallic particles. For a nonsaturating H_1, one can express $\chi'(\omega)$ and $\chi''(\omega)$[33]:

$$\chi_1(\omega)=a_1\chi'(\omega)+a_2\chi''(\omega),$$
$$\chi_2(\omega)=a_1\chi''(\omega)-a_2\chi'(\omega).$$

The ratio a_2/a_1 has been determined empirically by admixing $\chi_1(\omega)$ and $\chi_2(\omega)$ in order to symmetrize their

[31] C. Kittel and E. Abrahams, Phys. Rev. **90**, 238 (1953).

[32] R. E. Walstedt, Phys. Rev. **138**, A1096 (1965).

[33] A. C. Chapman, P. Rhodes, and E. F. W. Seymour, Proc. Phys. Soc. (London) **70B**, 345 (1957).

TABLE III. Experimental results and derived values of the spin-spin coupling constants in metallic platinum and lead. The value of $\delta\nu$ for Pt is deduced from the measured spin–spin relaxation time $T_2=1.1$ ms (Ref. 32).

Metal	Pt	Pb
$\delta\nu$ (kHz)	0.143	1.22±0.04
$2\tau_M$ (μsec)	480±10	305±15
J/B	6.1	2.2
$J/2\pi$ (kHz)	4.0±0.2	4.8±0.5
$\gamma^2\hbar/d^3$ calculated value (kHz)	0.265	0.124
$b/2\pi$ (kHz)	0.39±0.08	2.2±0.2

shapes. This correction is small and corresponds to $a_2/a_1=0.30$.

The obtained shape for $\chi''(\omega)$ is Lorentzian. The peak-to-peak width of $d\chi''/d\omega$ is found not to differ from that of $d\chi_2/d\omega$ which is $\Delta H=1.60\pm0.10$ G. This value agrees with the predicted results from measurements at 77 and 300°K.[16] In these last cases, T_1 contributed to the linewidth. There is also a good agreement with the observed value of the decay time of the echo envelope; $T_2=130\pm4$ μsec.

C. Values of the Coupling Constants

The two relationships for J and B can now be combined. The first is obtained from Fig. 3 and is given by the same curve for Pt ($c=0.33$) and Pb ($c=0.21$) on Fig. 9. It shows the variation of $J\tau_M$ versus the parameter J/B. In this coordinate system, the second relationship[20] becomes

$$J\tau_M/2\pi=(\delta\nu\tau_M/2.36\sqrt{c})\,(J/B)^2. \qquad (21)$$

This is a parabola, for which the coefficient depends upon the experimental values τ_M, $\delta\nu$, and c. The two cases of Pb and Pt are plotted in Fig. 9. The intercept of each parabola with the other curve yields the solutions for J/B and $J/2\pi$ given in Table III. There one also finds the calculated pure-dipolar coupling constants and the deduced value of the pseudodipole coupling constant $b/2\pi$.

As $J/B>1$ in both cases, one may remark that the use of the Anderson-Weiss model was justified. For Pt the value of J differs only by 5% from that derived with a simplified model.[11] The same conclusion is not valid for Pb, because of the low value of J/B. There the strength of both indirect spin–spin interactions is several times bigger than that derived earlier from a measurement of the second moment.[16] This is not surprising in view of the uncertainty of this last method.

V. DISCUSSION

This paper has shown that the shape of the spin-echo envelopes observed in alloys can be interpreted in terms of the model. Most features of the theoretical model have been checked in the experiments carried out with platinum and lead alloys. In both cases, the resonant nuclei have a spin $\frac{1}{2}$ so that these experiments could not test the quadrupolar effects. This method should thus be very useful in studying the electron-induced spin–spin interactions. It is complementary to to the steady-state methods. For lead and platinum, the Ruderman-Kittel and pseudodipolar coupling constants have been obtained.

The problem now is to relate these data to the electronic band structure in both metals. Unfortunately, the models at our disposal are very crude and allow only a qualitative discussion. For platinum it has been argued[34] that the main contribution to the indirect exchange coupling J is related to the s band. Thus, in this case, there is very little variation of J with the concentration of the alloy, in contrast with the drastic change of the Knight shift, the relaxation time T_1, and the susceptibility. Thus the present discussion will be limited to lead.

One may discuss the value of J on the basis of formula (16) which assumes a spherical Fermi surface and can be written for the case of first-nearest neighbors

$$\hbar J=[\Omega^2 m^*\xi^2 a^2(s)/8\pi\hbar^2 d^4]F(k_Fd),$$

where $F(k_Fd)=2k_Fd\cos(2k_Fd)-\sin(2k_Fd)$.

The simplest way to estimate $F(k_Fd)$ would be to take the free-electron value of the wave vector k_F. Unfortunately, it happens that this accidentally corresponds to a node of the function F. It is well known,[35] however, that a slight departure from a spherical Fermi surface will strongly affect the shape of this function. This certainly applied to lead.[36] As $2k_Fd$ is about equal to 11 or 12, one may take $F(k_Fd)$ to be of the order of 6. With the experimental value of J and $m^*=m$, an order of magnitude estimate for $\xi a(s)=0.5$ cm^{-1} is obtained. This is about two times bigger than the value derived from the Knight shift. For ξ close to unity, this is also in fair agreement with the value of $a(s)$ derived from optical spectra.[29] One will notice that the present theoretical calculations of nuclear indirect exchange interactions in metals are too simplified to allow a useful quantitative discussion in the case of lead. The same remark applies to the discussion of the strength of the pseudodipolar interactions. Qualitatively, the appreciable value of the ratio $b/J=0.45$ shows that the p character of the electronic wave function at the Fermi surface level exceeds the s character. It can be compared with $b/J=0.075$ obtained in metallic thallium,[4] which represented the only quantitatively studied case prior to the present work.

[34] C. Froidevaux, F. Gautier, and J. Weisman, *Proceedings of the International Conference on Magnetism, Nottingham, 1964* (Institute of Physics and The Physical Society, London, 1965), p. 390.

[35] G. Gousseland, J. Phys. Radium **23**, 928 (1962).

[36] J. R. Anderson and A. V. Gold, Phys. Rev. **139**, A1459 (1965).